INTERNATIONAL JOURNAL FOR NUMERICAL METHODS IN FLUIDS
Int. J. Numer. Meth. Fluids 2009; **59**:215–234
Published online 2 June 2008 in Wiley InterScience (www.interscience.wiley.com). DOI: 10.1002/fld.1821

Solution to transient Navier–Stokes equations by the coupling of differential quadrature time integration scheme with dual reciprocity boundary element method

C. Bozkaya and M. Tezer-Sezgin*, †

Department of Mathematics, Middle East Technical University, 06531 Ankara, Turkey

SUMMARY

The two-dimensional time-dependent Navier–Stokes equations in terms of the vorticity and the stream function are solved numerically by using the coupling of the dual reciprocity boundary element method (DRBEM) in space with the differential quadrature method (DQM) in time. In DRBEM application, the convective and the time derivative terms in the vorticity transport equation are considered as the nonhomogeneity in the equation and are approximated by radial basis functions. The solution to the Poisson equation, which links stream function and vorticity with an initial vorticity guess, produces velocity components in turn for the solution to vorticity transport equation. The DRBEM formulation of the vorticity transport equation results in an initial value problem represented by a system of first-order ordinary differential equations in time. When the DQM discretizes this system in time direction, we obtain a system of linear algebraic equations, which gives the solution vector for vorticity at any required time level. The procedure outlined here is also applied to solve the problem of two-dimensional natural convection in a cavity by utilizing an iteration among the stream function, the vorticity transport and the energy equations as well. The test problems include two-dimensional flow in a cavity when a force is present, the lid-driven cavity and the natural convection in a square cavity. The numerical results are visualized in terms of stream function, vorticity and temperature contours for several values of Reynolds (*Re*) and Rayleigh (*Ra*) numbers. Copyright © 2008 John Wiley & Sons, Ltd.

Received 29 May 2007; Revised 6 March 2008; Accepted 7 March 2008

KEY WORDS: DRBEM; DQM; transient Navier–Stokes equations; natural convection

*Correspondence to: M. Tezer-Sezgin, Department of Mathematics, Middle East Technical University, 06531 Ankara, Turkey.
†E-mail: munt@metu.edu.tr

Contract/grant sponsor: Scientific and Technical Research Council of Turkey

1. INTRODUCTION

The solution to the incompressible Navier–Stokes equations is the most significant area in computational fluid dynamics, which involves a wide range of applications in many branches of science and engineering. Four alternative formulations of the Navier–Stokes equations are given earlier. They are (i) the velocity–pressure formulation, (ii) the vorticity–stream function formulation, (iii) the stream function fourth-order equation and (iv) the velocity–vorticity formulation. Although, the velocity–pressure formulation gives the solution in terms of original primitive variables, for two-dimensional and also for axi-symmetric flows it is convenient to use the vorticity–stream function formulation where the equation of continuity is automatically satisfied and the number of equations to be solved is reduced. Of course, the resulting system consists of two coupled nonlinear equations. Aside from the fact that these coupled equations are nonlinear, there are several other difficulties associated with their solution. A major difficulty arises from the boundary conditions of the problem. In practice, only the velocity on the boundaries is prescribed, while for the numerical solution to the equation in the vorticity–stream function formulation we require the values of the vorticity on the boundaries as well. The advantage of using the velocity–pressure formulation is that we are dealing with the variables that have physical significance. However, in the velocity–pressure formulation it becomes necessary to solve a rather complicated pressure equation, introducing additional difficulties. A third possibility is to solve the fourth-order formulation of the Navier–Stokes equations. Although there is only one nonlinear equation that is to be solved, it must be realized that one is now faced with a higher-order nonlinear equation. One of the boundary conditions is given in terms of the normal derivatives, which also complicates the numerical procedure. Velocity–vorticity formulations of the incompressible Navier–Stokes equations have similar advantages over velocity–pressure formulations as the reduction in the number of equations to be solved through the elimination of the pressure. The problem of determining the vorticity boundary conditions also exists. The velocity field in turn must be determined from the vorticity field, which is the curl of the velocity field.

There are many studies on the numerical solutions to the Navier–Stokes equations in the above-mentioned formulations by using the boundary element method (BEM). A boundary-domain integral method is presented by Skerget and Rek [1] for solving Navier–Stokes equations in velocity–vorticity formulation. The solution is obtained by using 40 boundary elements and 100 internal cells for Re up to 400. Later, Ramsak and Skerget [2] have used mixed boundary elements in the same formulation of the Navier–Stokes equations. The subdomain-based BEM numerical scheme is developed by Ramsak and Skerget [3] for modelling two-dimensional unsteady laminar flow in stream function–vorticity form of the Navier–Stokes equations. Applications are on the steady backward facing step flow and a periodic flow past a circular cylinder. These direct applications of the BEM to the Navier–stokes equations lead to domain integrals that can be evaluated by using the cell integration approach. Although this method is effective and general, it makes the BEM lose its boundary-only nature, resulting in a time-consuming numerical scheme. One of the most popular methods to take the domain integrals to the boundary is the dual reciprocity method. The dual reciprocity BEM (DRBEM) approximates the nonlinear or nonhomogeneous terms of a partial differential equation as a series of vector-valued interpolation functions, and it yields a particular solution to the problem, which can be used together with Green's identity to convert the domain integrals to boundary integrals. Sarler and Kuhn [4] applied DRBEM to transient incompressible two-dimensional Navier–Stokes equations in primitive variables. As interpolation functions, thin plate splines are used and all derivatives involved are calculated through integral

DOI: 10.1002/fld

representation formulas. The classical lid-driven cavity problem at $Re = 100$ is solved. Later in Sarler *et al.* [5] DRBEM with constant, linear and quadratic elements is applied to the solution of a steady natural convection problem in porous media. The DRBEM is improved by using the domain decomposition technique by Florez and Power [6] to solve the Navier–Stokes equations at moderate Reynolds numbers. They introduce a radial basis function interpolation scheme for the velocity field, which satisfies the continuity equation (mass conservative). The DRBEM is also used by Rahaim and Kassab [7] for solving incompressible, laminar, viscous fluid flow and heat transfer problems. The DRBEM with subdomain decomposition approach for two-dimensional Navier–Stokes equations [8] and for two-dimensional thermal convection flow problems [9] is utilized and the solutions are obtained for Reynolds number up to 600 and Rayleigh number up to 10^4, respectively.

Ingber and Kempka [10] and Brown and Ingber [11] have used a vorticity formulation for the analysis of incompressible viscous fluid flow problems with the driven-cavity benchmark problem for *Re* 100 and 400, respectively. To more accurately satisfy both components of the velocity boundary conditions, a Galerkin formulation is applied to the generalized Helmholtz decomposition and vorticity equation is solved using a Galerkin finite element method where a parallelization is utilized in their latter study. Ingber [12] extended this vorticity formulation to study the natural convection flows in differentially heated enclosures.

Researches have also been carried out for solving viscous flows at high Reynolds numbers. From these we can count the studies of Zhao and Liao [13] and Wu and Liao [14], which are general BEM solutions in a driven cavity with *Re* values up to 7500. A parallel computation is used in [13], whereas both parallelization and domain decomposition are used in [14] to reduce the CPU time. There are some other numerical schemes used for solving Navier–Stokes equations at high Reynolds numbers for lid-driven cavity problem and also for two-dimensional natural convection flow in a square cavity. Sahin and Owens [15] described an implicit cell-vertex finite volume method for the solution to the Navier–Stokes equations at high Reynolds numbers. They eliminate the pressure term by multiplying the momentum equations with the unit normal to a control boundary. They have used quite a fine mesh as 257×257 for increasing values of *Re* number up to 10 000 for lid-driven cavity. The lid-driven cavity flow is also solved by parallel lattice Boltzmann method using the multi-relaxation-time scheme by Wu and Shao [16]. Solution is obtained for values of *Re* number up to 7500 by using 256×256 lattice points. Wong and Chan [17] have given numerical verifications of the mixed finite element consistent splitting scheme for solving Navier–Stokes equations in primitive variables. Their numerical simulation is for the double lid-driven cavity by using fine mesh with 513×513 points for high Reynolds number. The Navier–Stokes equations in stream function–vorticity formulation have been solved using a fine uniform grid mesh of 601×601 for high *Re* number by Erturk *et al.* [18]. Sousa and Sobey [19] have developed a global iteration matrix formulation for the stream function–vorticity equations for examining the effect on numerical stability of boundary vorticity discretization. Two-dimensional time-dependent incompressible Navier–Stokes equations in stream function–vorticity formulation have been solved by uncoupling the variables linearizing the advective terms and using Euler-type implicit time discretization by Ghadi *et al.* [20]. A numerical solution by using differential quadrature method (DQM) has been developed by Lo *et al.* [21] for two-dimensional Navier–Stokes equations in velocity–vorticity form and this numerical algorithm has been implemented to study natural convection in a differentially heated cavity. For the time derivative, an iterative second-order time stepping of finite difference type has been used. Ding *et al.* [22] also presented a mesh-free finite difference scheme based on the use of a weighted least-square approximation

DOI: 10.1002/fld

to solve two-dimensional natural convection in a square cavity. Moreover, the global method of generalized differential quadrature has been applied to simulate the natural convection in a square cavity by Shu and Xue [23]. In these two studies also iterative time integration schemes have been used.

Most of the studies on the discretization of time derivative in the vorticity transport equation are based on finite difference approximations. Erturk *et al.* [18] and Ingber and co-workers [10–12] used an implicit Euler time scheme, which is first-order accurate; Skerget and Rek [1], Ramsak and Skerget [3] used forward difference approximation for the time derivative of vorticity; and Wong and Chan [17] used a fully implicit second-order backward differentiation formula since it is stable. Kobayashi and Pereira [24] have chosen an explicit fourth-order accurate Runge–Kutta method for solving the unsteady fourth-order stream function equation. It is known that the above-mentioned methods need iterations with a proper choice of time increment Δt for obtaining the solution at a required time level. Since all the equations obtained from space discretization must be solved in each iteration, the whole solution procedure is usually computationally expensive.

In this paper, we follow the stream function–vorticity formulation of the Navier–Stokes equations and use the DRBEM treating the time derivatives and the nonlinear terms as the nonhomogeneity in the vorticity transport and the energy equations. In the stream function equation the nonhomogeneity is the previous value of vorticity and these three equations are solved iteratively. We obtain the vorticity boundary conditions from the Taylor series expansion of stream function equation in terms of boundary and interior stream function values. The approximations for the vorticity boundary conditions affect the accuracy and convergence of the whole solution procedure. The formula we use involves the unknown values of stream function at the distances ph and qh away from the boundary (p and q are integers and h is the mesh distance). The DRBEM applications to vorticity transport and energy equations result in systems of first-order initial value problems in time. We have made use of the DQM in discretizing the time derivatives in these initial value problems since it is known that DQM is unconditionally stable [25]. The DQM gives the solution at any required time level at one stroke with a minimal number of discretized points between the initial level and the required time level. By taking these results as initial values we solve the system for obtaining the solution at another required time level. In this manner, we reach iteratively to the steady state by solving the system in time blocks. These time blocks are discretized with very small number of Gauss–Chebyshev–Lobatto (GCL) points since it is known that it gives better accuracy than the use of equally spaced points [25]. The use of the DQM for the time derivative has been used with success in solving transient convection–diffusion and unsteady MHD equations [26, 27]. We extend this idea now for the solution to unsteady Navier–Stokes and energy equations. Our solution procedure has been tested first on solving Navier–Stokes equations when a force term is present for which an exact solution is available. Then, the lid-driven cavity and natural convection cavity problems are solved for Reynolds number up to 1000 and Rayleigh number up to 10^5, respectively. These two benchmark problems have attracted the attention of many scientists in developing computational algorithms for solving the Navier–Stokes and energy equations.

2. BASIC EQUATIONS

A two-dimensional laminar flow of an incompressible viscous fluid is governed by the Navier–Stokes equations, which are given in the nondimensional form in terms of momentum

DOI: 10.1002/fld

equations:

$$\begin{aligned}\frac{\partial u}{\partial t}+u\frac{\partial u}{\partial x}+v\frac{\partial u}{\partial y}&=-\frac{\partial p}{\partial x}+\frac{1}{Re}\nabla^2 u\\ \frac{\partial v}{\partial t}+u\frac{\partial v}{\partial x}+v\frac{\partial v}{\partial y}&=-\frac{\partial p}{\partial y}+\frac{1}{Re}\nabla^2 v\end{aligned} \tag{1}$$

and the continuity equation:

$$\frac{\partial u}{\partial x}+\frac{\partial v}{\partial y}=0 \tag{2}$$

where $u=u(x,y,t)$ and $v=v(x,y,t)$ are the components of the velocity field, $p=p(x,y,t)$ is the pressure and Re is the Reynolds number of the flow.

Introducing the vorticity field with the z-component $w=\partial v/\partial x-\partial u/\partial y$, the momentum equations provide a vorticity transport equation:

$$\frac{1}{Re}\nabla^2 w=\frac{\partial w}{\partial t}+u\frac{\partial w}{\partial x}+v\frac{\partial w}{\partial y} \tag{3}$$

A stream function is defined satisfying the continuity condition as

$$\frac{\partial \psi}{\partial x}=-v,\quad \frac{\partial \psi}{\partial y}=u \tag{4}$$

which is connected to the vorticity w by a Poisson equation

$$\nabla^2\psi=-w \tag{5}$$

3. METHOD OF SOLUTION

The Navier–Stokes equations are coupled in terms of vorticity and stream function as shown in Equations (3) and (5). These coupled nonlinear equations can be solved iteratively. In the solution procedure, first the Poisson equation (5) is solved for the stream function with an initial vorticity estimate by using the DRBEM. After obtaining the stream function values for both boundary and interior nodal points, the x and y derivatives of stream function are found by approximating the stream function with a radial basis function. When we insert these derivative values in the vorticity transport equation (3), it turns out to be a linear transient convection–diffusion equation with constant coefficients. Then, the combination of the DRBEM in spatial domain and DQM in time domain is used for the solution.

3.1. Application of DRBEM to vorticity transport and stream function equations

The DRBEM is employed to transform the vorticity transport equation (3) and the stream function equation (5) into boundary integral equations by using the fundamental solution to the Laplace equation and treating the terms on the right-hand sides of these equations as the nonhomogeneity. Thus, Equations (3) and (5) are weighted through the domain Ω of the problem as in [28], by the fundamental solution u^* of Laplace equation in two dimensions. Then by using Green's second

DOI: 10.1002/fld

identity, we have

$$\frac{1}{Re}c_i w_i + \int_\Gamma \frac{1}{Re}\left(q^* w - u^* \frac{\partial w}{\partial n}\right) \mathrm{d}\Gamma = -\int_\Omega \left(\frac{\partial w}{\partial t} + u\frac{\partial w}{\partial x} + v\frac{\partial w}{\partial y}\right) u^* \,\mathrm{d}\Omega \tag{6}$$

and

$$c_i \psi_i + \int_\Gamma \left(q^* \psi - u^* \frac{\partial \psi}{\partial n}\right) \mathrm{d}\Gamma = -\int_\Omega (-w) u^* \,\mathrm{d}\Omega \tag{7}$$

where subscript i denotes the source point, $q^* = \partial u^*/\partial n$ and Γ is the boundary of the domain Ω. The constant $c_i = \theta_i/2\pi$ with the internal angle θ_i at the source point i.

In order to obtain boundary integrals that are equivalent to the domain integrals in Equations (6) and (7), a dual reciprocity approximation is introduced. The basic idea is to expand the terms described as nonhomogeneity in the form

$$\frac{\partial w}{\partial t} + u\frac{\partial w}{\partial x} + v\frac{\partial w}{\partial y} = \sum_{j=1}^{N+L} \alpha_j(t) f_j(x, y) \tag{8}$$

and

$$-w = \sum_{j=1}^{N+L} \tilde{\alpha}_j f_j(x, y) \tag{9}$$

for Equations (6) and (7), respectively. The above series involve a set of radial basis (coordinate) functions $f_j(x, y)$ that are dependent only on geometry and they are linked with the particular solutions $\hat{u}_j$ to the equation $\nabla^2 \hat{u}_j = f_j$. The unknown coefficients α_j are time dependent whereas $\tilde{\alpha}_j$ are undetermined constants. The numbers of boundary and selected internal nodes are denoted by N and L, respectively. Then, the application of the DRBEM leads to the following boundary integral equations:

$$\frac{1}{Re}c_i w_i + \int_\Gamma \frac{1}{Re}\left(q^* w - u^* \frac{\partial w}{\partial n}\right) \mathrm{d}\Gamma = \sum_{j=1}^{N+L} \alpha_j(t) \left[c_i \hat{u}_{ji} + \int_\Gamma (q^* \hat{u}_j - u^* \hat{q}_j)\,\mathrm{d}\Gamma\right] \tag{10}$$

and

$$c_i \psi_i + \int_\Gamma \left(q^* \psi - u^* \frac{\partial \psi}{\partial n}\right) \mathrm{d}\Gamma = \sum_{j=1}^{N+L} \tilde{\alpha}_j \left[c_i \hat{u}_{ji} + \int_\Gamma (q^* \hat{u}_j - u^* \hat{q}_j)\,\mathrm{d}\Gamma\right] \tag{11}$$

where $\hat{q}_j = \partial \hat{u}_j/\partial n$.

When constant elements are used for the approximation of ψ, w and their normal derivatives on the boundary, the matrix–vector forms of the resulting DRBEM formulation of the vorticity transport and stream function equations are obtained, respectively, as

$$\frac{1}{Re}\left(Hw - G\frac{\partial w}{\partial n}\right) = (H\hat{U} - G\hat{Q})\alpha \tag{12}$$

and

$$H\psi - G\frac{\partial \psi}{\partial n} = (H\hat{U} - G\hat{Q})\tilde{\alpha} \tag{13}$$

DOI: 10.1002/fld

where G and H are the square matrices whose coefficients are calculated by integrating u^* and q^* over each boundary element. Thus, the entries of these matrices are given by

$$H_{ij} = c_i \delta_{ij} + \frac{1}{2\pi} \int_{\Gamma_j} \frac{\partial}{\partial n} \left(\ln \left(\frac{1}{r} \right) \right) \mathrm{d}\Gamma_j$$

$$G_{ij} = \frac{1}{2\pi} \int_{\Gamma_j} \ln \left(\frac{1}{r} \right) \mathrm{d}\Gamma_j$$

where r is the modulus of the distance vector from point i to element j, δ_{ij} is the Kronecker delta function and Γ_j is the boundary of the jth element. Matrices $\hat{U}$ and $\hat{Q}$ are constructed by taking each of the vectors $\hat{u}_j$ and $\hat{q}_j$ as columns, respectively.

By evaluating expressions (8) and (9) at all boundary nodes and inverting, the matrix–vector equations (12) and (13) will have the form

$$\frac{1}{Re} \left(Hw - G \frac{\partial w}{\partial n} \right) = (H\hat{U} - G\hat{Q}) F^{-1} \left\{ \frac{\partial w}{\partial t} + u \frac{\partial w}{\partial x} + v \frac{\partial w}{\partial y} \right\} \tag{14}$$

and

$$H\psi - G \frac{\partial \psi}{\partial n} = (H\hat{U} - G\hat{Q}) F^{-1} \{-w\} \tag{15}$$

where $(N+L) \times (N+L)$ matrix F contains the coordinate functions f_j's as columns.

Observe that the resulting DRBEM discretization produces nonlinear and coupled equations in vorticity and stream function because of relationship (4). Thus, an iterative procedure is necessary to solve them. The iterative procedure proposed here reduces Equation (14) to a set of ordinary differential equations in time and Equation (15) to a system of linear algebraic equations in each iteration.

We shall now describe the iterative procedure:

(i) Start with some initial approximations for the vorticity, namely w^0.

(ii) Solve the stream function equation appearing in Equation (15) with $w = w^0$. By this initial vorticity guess the right-hand side of Equation (15) produces a constant vector. Moreover, by the insertion of the boundary conditions for the stream function and its normal derivative and by the rearrangement of Equation (15), we end up with a linear system of equations

$$\tilde{A}\tilde{\psi} = \tilde{b} \tag{16}$$

where $\tilde{A}$ is the coefficient matrix of size $(N+L) \times (N+L)$, $\tilde{b}$ is a known vector and $\tilde{\psi}$ is the solution vector containing N boundary values of ψ and $\partial\psi/\partial n$ plus L interior values of ψ.

(iii) Once the values of stream functions are obtained both on the boundary and inside of the domain, the x and y derivatives of stream function can also be approximated by using the same coordinate functions $f_j(x, y)$, i.e.

$$\psi = \sum_{j=1}^{N+L} \tilde{\beta}_j f_j(x, y) \tag{17}$$

DOI: 10.1002/fld

where $\tilde{\beta}_j$ are unknown coefficients and this equation can be rewritten as

$$\psi = F\tilde{\beta} \tag{18}$$

Differentiating Equation (18), we have

$$\frac{\partial \psi}{\partial x} = \frac{\partial F}{\partial x} F^{-1}\psi, \quad \frac{\partial \psi}{\partial y} = \frac{\partial F}{\partial y} F^{-1}\psi \tag{19}$$

since $\tilde{\beta}_j = F^{-1}\psi$. Thus, the velocity components u and v given in Equation (4) in terms of the derivatives of stream function at the required nodal points can be found by using Equation (19). These obtained values of u and v will be used as constants in the solution to vorticity transport equation.

(iv) Solve the vorticity transport equation (14). Since Equation (14) involves $\partial w/\partial t$, the vorticity is approximated by using the same coordinate function $f_j(x, y)$ as

$$w = \sum_{j=1}^{N+L} \beta_j(t) f_j(x, y) \tag{20}$$

where $\beta_j(t)$'s are time-dependent unknown coefficients and the system $w = F\beta$ leads to the convective terms of the vorticity

$$\frac{\partial w}{\partial x} = \frac{\partial F}{\partial x} F^{-1} w, \quad \frac{\partial w}{\partial y} = \frac{\partial F}{\partial y} F^{-1} w \tag{21}$$

Substituting convection terms back into Equation (14), one can obtain the system of ordinary differential equations

$$C\dot{w} + \tilde{H}w - \tilde{G}\frac{\partial w}{\partial n} = 0 \tag{22}$$

where matrices C, $\tilde{H}$ and $\tilde{G}$ are given by

$$\begin{aligned} C &= -(H\hat{U} - G\hat{Q})F^{-1} \\ \tilde{H} &= \frac{1}{Re}H + CR_1 + CR_2 \\ \tilde{G} &= \frac{1}{Re}G \end{aligned} \tag{23}$$

and

$$R_1 = u\frac{\partial F}{\partial x}F^{-1}, \quad R_2 = v\frac{\partial F}{\partial y}F^{-1} \tag{24}$$

Now, from Equation (22), the standard form of the first-order initial value problem

$$\dot{w} + Bw = D\frac{\partial w}{\partial n} \tag{25}$$

is obtained, in which $B = C^{-1}\tilde{H}$, $D = C^{-1}\tilde{G}$ and superscript dot denotes the time derivative. Then, system (25) is integrated in time using a DQM, which enables us to obtain vorticity values at any required time level.

DOI: 10.1002/fld

(v) Repeat steps (ii)–(iv) either until the steady state or a required time level is reached. In our calculations we terminate the procedure when the difference between the values of ψ and w at two successive iterates in L_∞ norm is less than a preassigned tolerance.

3.2. Application of the DQM to vorticity transport equation

The DQM approximates the derivative of a smooth function at a grid point by a linear weighted summation of all the functional values in the whole computational domain [25]. In this study DQM is employed to discretize the time derivative of w in Equation (25) [26, 27].

The DQM analogue of the first-order derivative of a function $f(t)$ at a grid point t_i can be expressed as

$$\left.\frac{\mathrm{d}f(t)}{\mathrm{d}t}\right|_{t_i} = \sum_{j=1}^{M} a_j(t_i) f(t_j) \tag{26}$$

where $i = 1, 2, \ldots, M$ is the number of grid points t_i in the time direction and $a_j(t_i)$ are the weighting coefficients for derivative approximations of $f(t)$ to be determined by the polynomial-based DQM [25, 29].

The weighting coefficients for the first-order derivative are given as

$$a_{ij} = \frac{M^{(1)}(t_i)}{(t_i - t_j) M^{(1)}(t_j)}, \quad i \neq j, \;\; i, j = 1, 2, \ldots, M \tag{27}$$

$$a_{ii} = -\sum_{j=1, j\neq i}^{M} a_j(t_i) \tag{28}$$

where

$$M^{(1)}(t_j) = \prod_{k=1, k\neq j}^{M} (t_j - t_k) \tag{29}$$

and

$$a_{ij} = a_j(t_i)$$

By using the DQM time approximation, the first-order initial value problem (25) becomes

$$\sum_{j=1}^{M} a_{ij} W_j + B W_i = D q_i, \quad i = 1, 2, \ldots, M \tag{30}$$

where the vectors W_i and q_i are in fact the w and $\partial w/\partial n$ vectors, respectively, at the ith time level and they are given as

$$\begin{aligned} W_i &= \{w_{1i}, w_{2i}, \ldots, w_{Ni}, w_{(N+1)i}, \ldots, w_{(N+L)i}\} \\ q_i &= \left\{ \left.\frac{\partial w}{\partial n}\right|_{1i}, \left.\frac{\partial w}{\partial n}\right|_{2i}, \ldots, \left.\frac{\partial w}{\partial n}\right|_{Ni}, 0, \ldots, 0 \right\} \end{aligned} \tag{31}$$

in which $w_{ji} = w_j(t_i)$ and $\partial w/\partial n|_{ji} = \partial w/\partial n|_j(t_i)$.

DOI: 10.1002/fld

Equation (30) gives a system of linear equations for each time level t_i, which can be denoted in a matrix–vector form

$$S\tilde{W} = \tilde{D}\tilde{q} \tag{32}$$

where

$$S = A + \tilde{B} \tag{33}$$

Matrices A, $\tilde{B}$ and $\tilde{D}$ are expressed as

$$A = \begin{bmatrix} \bar{a}_{11} & \bar{a}_{12} & \dots & \bar{a}_{1M} \\ \bar{a}_{21} & \bar{a}_{22} & \dots & \bar{a}_{2M} \\ \vdots & & & \\ \bar{a}_{M1} & \bar{a}_{M2} & \dots & \bar{a}_{MM} \end{bmatrix} \tag{34}$$

with $(N+L)\times(N+L)$ submatrices $\bar{a}_{ij}$ defined as

$$\bar{a}_{ij} = a_{ij} I$$

and

$$\tilde{B} = \begin{bmatrix} B & & & \\ & B & & \\ & & \ddots & \\ & & & B \end{bmatrix}, \quad \tilde{D} = \begin{bmatrix} D & & & \\ & D & & \\ & & \ddots & \\ & & & D \end{bmatrix} \tag{35}$$

The sizes of matrices S, $\tilde{B}$, A and $\tilde{D}$ are $(N+L)M\times(N+L)M$ and the identity matrix I is of size $(N+L)\times(N+L)$.

The $(N+L)M\times 1$ vectors $\tilde{W}$ and $\bar{q}$ are defined as

$$\tilde{W} = \{w_{11}, w_{21}, \dots, w_{(N+L)1}; w_{12}, w_{22}, \dots, w_{(N+L)2}; \dots; w_{1M}, w_{2M}, \dots, w_{(N+L)M}\} \tag{36}$$

$$\bar{q} = \left\{ \left.\frac{\partial w}{\partial n}\right|_{11}, \left.\frac{\partial w}{\partial n}\right|_{21}, \dots, \left.\frac{\partial w}{\partial n}\right|_{N1}, 0, \dots, 0; \left.\frac{\partial w}{\partial n}\right|_{12}, \dots, \left.\frac{\partial w}{\partial n}\right|_{N2}, 0, \dots, 0; \right.$$
$$\left. \dots; \left.\frac{\partial w}{\partial n}\right|_{1M}, \dots, \left.\frac{\partial w}{\partial n}\right|_{NM}, 0, \dots, 0 \right\} \tag{37}$$

In the linear system (32) boundary conditions (some of $\tilde{W}$ and some of $\tilde{q}$ nodal specified values) are inserted by interchanging the negative of corresponding columns and reordering the solution vector in terms of unknown $\tilde{W}$ and $\tilde{q}$ nodal values. When the initial condition is also inserted at the interior plus boundary nodes for the initial time level, system (32) finally becomes a rectangular system since known initial $\tilde{W}$ values are passed to the right-hand side leaving less number of unknowns than the number of equations.

The resulting reordered form of system (32) is given as

$$\tilde{S}X = b \tag{38}$$

DOI: 10.1002/fld

where the size of matrix $\tilde{S}$ is $((N+L)M-L)\times((N+L)M-L)$. Vectors X and b have the size $((N+L)M-L)\times 1$ if the boundary condition is of Dirichlet type. For Neumann type of boundary conditions, the sizes of $\tilde{S}$, X and b are appropriately arranged. Vector X contains the unknown values of w and its normal derivative for each nodal points at all the required time levels, whereas vector b contains all boundary plus initial information. Therefore, once system (38) is solved, one can obtain the solution for vorticity on the entire domain at any time level at one stroke and then iteratively at steady state.

4. NUMERICAL RESULTS

We consider three test problems. As a first example, the Navier–Stokes equation in a square domain ($0\leqslant x, y\leqslant 1$) when an external force is present is solved to see the accuracy and efficiency of our numerical method since the exact solution is available. The second example is the lid-driven cavity problem for which the fluid in the cavity is driven by the motion of one of the walls with a constant velocity. In the DRBEM discretization for the spatial domains, we use a suitable number of constant boundary elements and some interior nodes for presenting the solution in terms of graphics. For the time domain GCL points are used in the differential quadrature discretization. Since the DQM is unconditionally stable we are allowed to use arbitrarily large time step size in each time block. Thus, the number of time discretization points, M, can be quite small. A suitable number of the internal points, L, is taken to depict the behaviour of the solution. The two-dimensional natural convection problem in a square cavity is also solved as a third application with the proposed iterative procedure. Now, the Navier–Stokes equations include the buoyancy force generated as a result of fluid density difference caused by the temperature difference. The buoyancy term is computed based on the Boussinesq approximation.

4.1. Navier–Stokes equations in a square

The aim of this first problem is to verify the accuracy of the proposed method. The equations now include a force term f as

$$\begin{gathered}\frac{\partial w}{\partial t}+u\frac{\partial w}{\partial x}+v\frac{\partial w}{\partial y}=\frac{1}{Re}\nabla^2 w+f\\ \nabla^2\psi=w\end{gathered}\tag{39}$$

with no slip boundary conditions (i.e. $\psi|_\Gamma=0$) and $\partial\psi/\partial n|_\Gamma=0$, where Γ is the boundary of the square domain $0\leqslant x, y\leqslant 1$. Here the velocity field is given by $u=-\partial\psi/\partial y$ and $v=\partial\psi/\partial x$. The vorticity boundary conditions are taken from the exact solution

$$\begin{aligned}\psi &= -\sin t\sin^2\pi x\sin^2\pi y\\ w &= -\pi^2\sin t(\cos 2\pi x+\cos 2\pi y-2\cos 2\pi x\cos 2\pi y)\\ u &= \pi\sin t\sin 2\pi y\sin^2\pi x\\ v &= -\pi\sin t\sin 2\pi x\sin^2\pi y\end{aligned}\tag{40}$$

DOI: 10.1002/fld

and the force is given by

$$f = -\pi^2 \cos t(\cos 2\pi x + \cos 2\pi y - 2\cos 2\pi x \cos 2\pi y) + \pi^4 \sin^2 t \sin 2\pi x \sin 2\pi y(\cos 2\pi x - \cos 2\pi y) - \frac{4}{Re}\pi^4 \sin t(\cos 2\pi x + \cos 2\pi y - 4\cos 2\pi x \cos 2\pi y) \quad (41)$$

In the DRBEM discretization we use N constant boundary elements ranging from $N=64$ to 80 and $M=4$ GCL points are taken in the time discretization for DQM. In Figures 1–3 the agreement of our numerical solutions with the exact solution is depicted for both the stream function and the

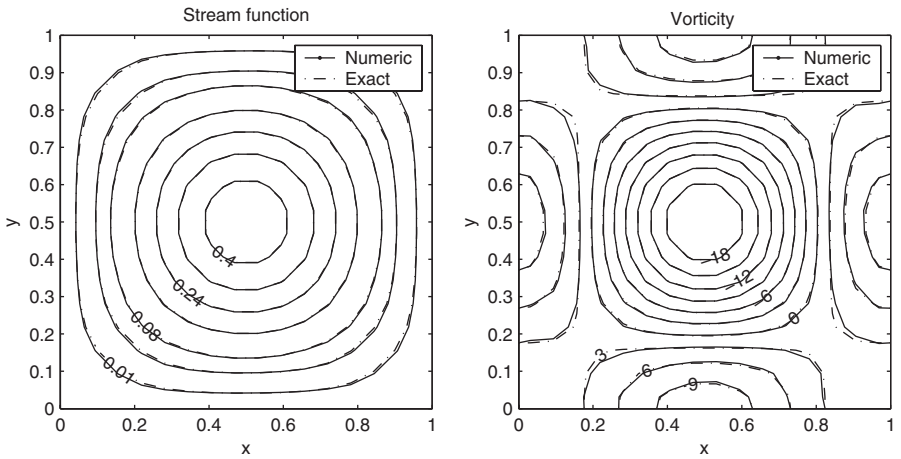

Figure 1. Stream function and vorticity contours for $Re=500$, $N=64$, $M=4$, $T=10$.

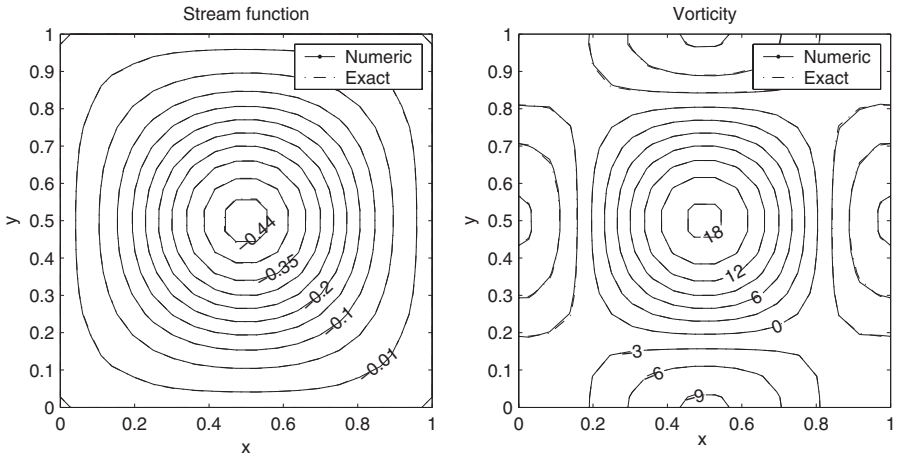

Figure 2. Stream function and vorticity contours for $Re=1500$, $N=72$, $M=4$, $T=0.5$.

DOI: 10.1002/fld

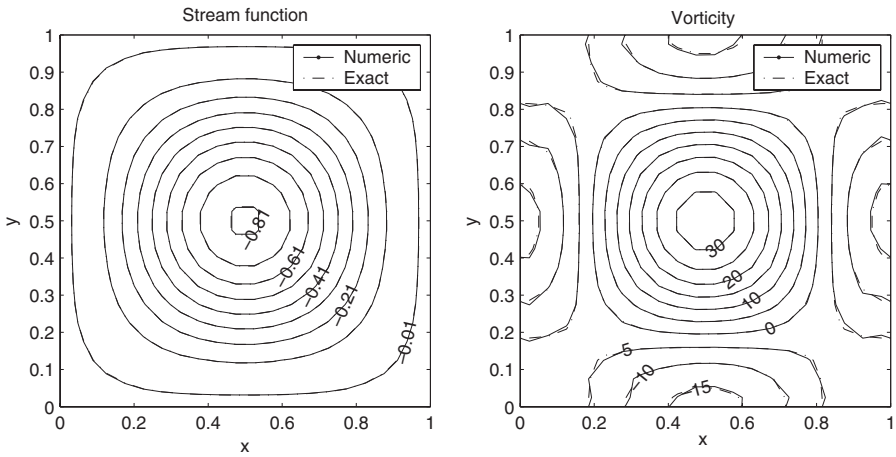

Figure 3. Stream function and vorticity contours for $Re=2000$, $N=80$, $M=4$, $T=1$.

vorticity in terms of contours at several time levels for the Reynolds number $Re=500$, 1500 and 2000, respectively. It is noted that this viscous flow problem has the particularity of having a flow pattern, which is independent of the Reynolds number.

4.2. Lid-driven cavity flow

The second problem is the classical lid-driven cavity flow in a square domain $\Omega=[0,1]\times[0,1]$ containing a recirculating flow induced by the motion of the lid.

We consider the equations governing the transient, laminar flow of a viscous incompressible fluid in a square cavity. The fluid in the cavity is driven by the motion of the upper wall, which is assumed to move with a constant velocity $u=-1$. The governing equations are the same with the previous problem where the load $f=0$. The velocities and the stream function are prescribed on the boundaries of the square cavity (Figure 4) bounded by three motionless walls and by a fourth wall moving in its own plane.

These boundary conditions are used for the solution to the stream function. In order to solve the vorticity transport equation, vorticity boundary conditions are required and these values can be approximated from the discretized stream function equation using the relation

$$w_{i,j}=-\nabla^2\psi_{i,j} \tag{42}$$

The boundary approximation for w is obtained on any boundary by taking

$$\psi_{nn}|_0=\alpha_0\psi_0+\alpha_1\psi_p+\alpha_2\psi_q+\alpha_3\psi_n|_0 \tag{43}$$

where subscripts 0, p and q indicate ψ values on the boundary mesh point, ph and qh distances away from the boundary, respectively. The expansion of ψ_p and ψ_q into Taylor series about the mesh point numbered 0 and reorganization of terms gives

$$\psi_{nn}|_0=\psi_0(\alpha_0+\alpha_1+\alpha_2)+\psi_n|_0(ph\alpha_1+qh\alpha_2+\alpha_3)+\psi_{nn}|_0\left(\frac{p^2h^2}{2}\alpha_1+\frac{q^2h^2}{2}\alpha_2\right)+\cdots \tag{44}$$

DOI: 10.1002/fld

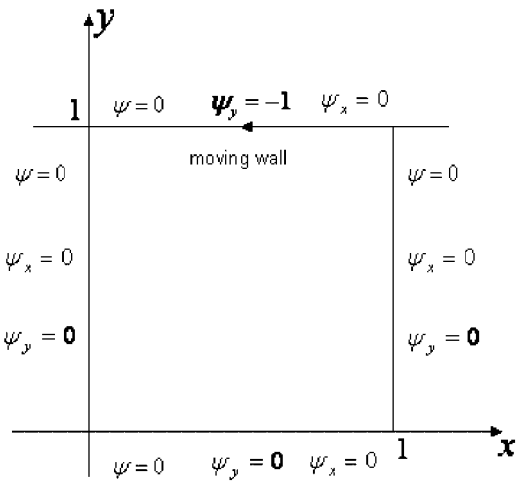

Figure 4. Boundary conditions for the lid-driven cavity problem.

In this latter equality, by setting the corresponding terms equal we obtain the solution

$$\alpha_0 = \frac{-2(p^3-q^3)}{h^2p^2q^2(p-q)}, \quad \alpha_1 = \frac{-2q}{h^2p^2(p-q)}, \quad \alpha_2 = \frac{-2p}{h^2q^2(p-q)}, \quad \alpha_3 = \frac{-2(p+q)}{hpq} \tag{45}$$

where p and q are positive integers and $p \neq q$. Thus, the boundary approximation becomes

$$w_0 = -h^{-2}\left[-\frac{2(p^3-q^3)}{p^2q^2(p-q)}\psi_0 - \frac{2q}{p^2(p-q)}\psi_p + \frac{2p}{q^2(p-q)}\psi_q - \frac{2h(p+q)}{pq}\psi_n|_0\right] \tag{46}$$

which involves the unknown ψ values at distances ph and qh along the normal and has a truncation error of order h^2. Since boundary values of ψ, ψ_x, ψ_y for the cavity flow are given, the boundary values of w can be obtained from Equation (46).

In the computations $p=2$ and $q=1$ are taken. We use $N=56$, 88 and 112 constant boundary elements and $M=3$, 2 and 2 time discretization points in each time block for the values of Reynolds number $Re=100$, 500 and 1000, respectively. The steady-state stream function and the vorticity values are obtained after 59, 116 and 200 iterations with an accuracy of 10^{-4} for the Reynolds number $Re=100$, 500 and 1000 and these results are presented, respectively, in the Figures 5–7.

At a Reynolds number of around 100, the streamline primary vortex moves towards the left-hand wall. At Reynolds numbers of 500 and 1000 the primary vortex starts to move towards the cavity centre. As the Reynolds number increases up to 500, the recirculations appear at the lower corners for the streamlines. At $Re=1000$ the recirculation close to the upper right corner shows up since the fluid movement is affected by the velocity of the lid that moves to the left. As Re increases the vorticity contours move away from the cavity centre towards the cavity walls indicating that strong vorticity gradients develop on the lid and the cavity walls (especially $x=0$ wall). The fluid begins to rotate with a constant angular velocity. These behaviours are in good agreement with the behaviours observed in [15, 16, 20]. Figures 8 and 9 show the velocity profiles for u along the vertical line ($x=0.5$) and v along the horizontal line ($y=0.5$) passing through the geometric

DOI: 10.1002/fld

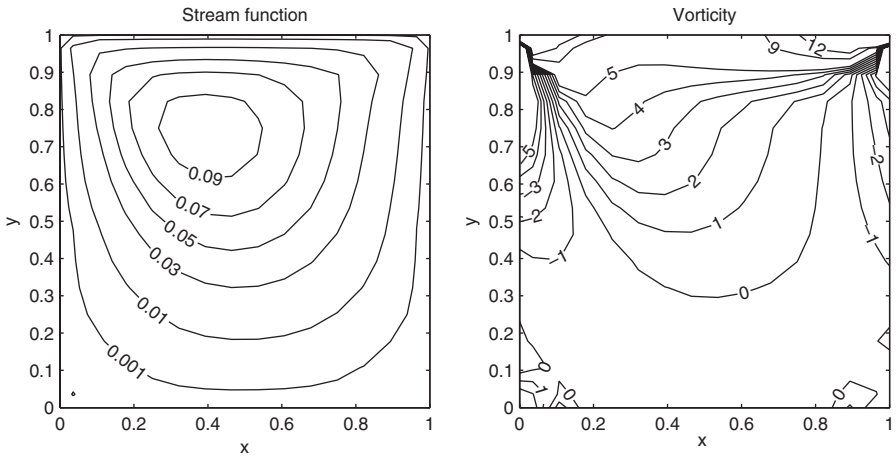

Figure 5. Stream function and vorticity contours for $Re=100$, $N=56$, $M=3$.

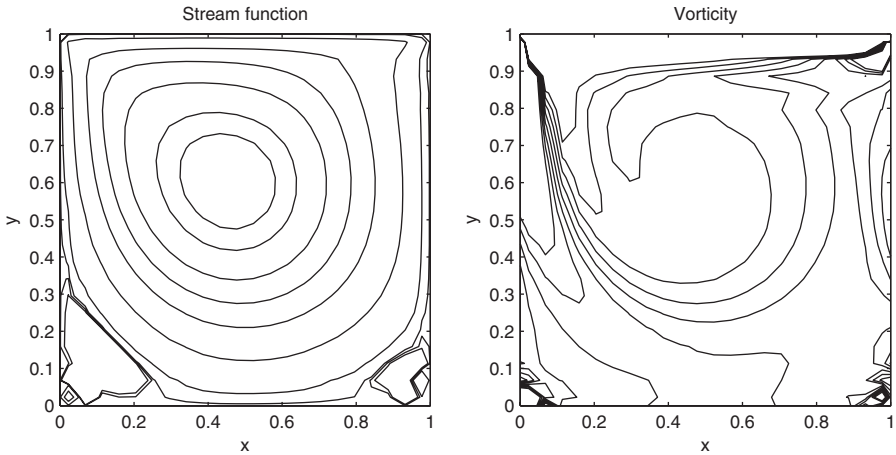

Figure 6. Stream function and vorticity contours for $Re=500$, $N=88$, $M=2$.

centre of the cavity for the values of Reynolds number $Re=100$ and 400. The numerical results obtained by the coupling of the DRBEM and DQM are compared with the results of Ghia [30] (by taking $u=1$ on the upper lid as is done in [30]) and it is observed that they are in good agreement.

The numbers of the boundary elements N and the time points M for one time block are so small that the whole procedure is still more economical than the FDM, which has to use very small time increment for stability. Although there is no certain relationship between N, M and L on the accuracy and the convergence of the numerical solution, one should be careful about the choice of N, M and L for not having an oversized final linear system of equations for the solution. Thus, the application of the present method to the three-dimensional problems is not recommended since one has to deal with much larger matrices.

DOI: 10.1002/fld

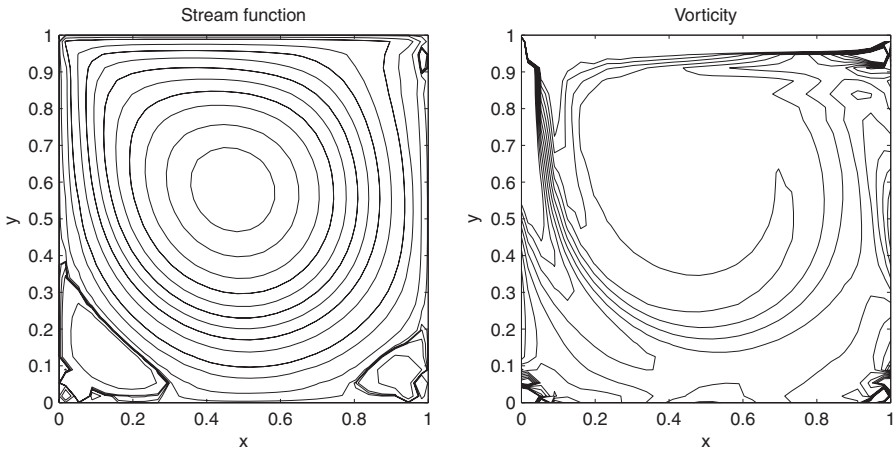

Figure 7. Stream function and vorticity contours for $Re = 1000$, $N = 112$, $M = 2$.

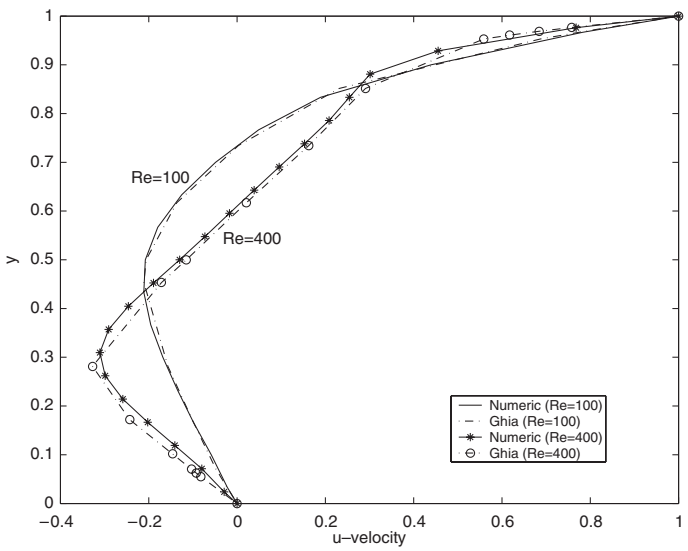

Figure 8. u-velocity along the vertical line ($x = 0.5$).

4.3. Natural convection in a square cavity

Natural convection in a differentially heated enclosure, which is a popular problem as testing any proposed numerical scheme, is added here since the governing equations can be treated easily with the proposed method in this paper. The vorticity transport equation is coupled to the energy equation through the buoyancy force $RaPr\partial T/\partial x$ and the energy equation is exactly in the same form (convection terms multipliers are the velocity components) of vorticity transport equation for the Navier–Stokes equations.

DOI: 10.1002/fld

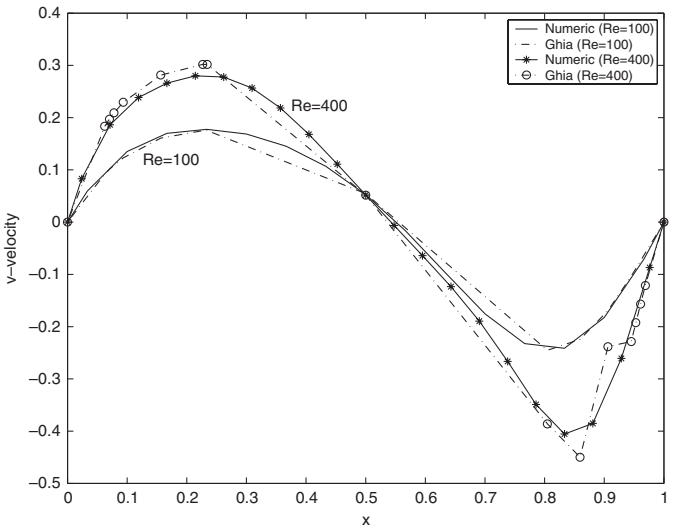

Figure 9. v-velocity along the horizontal line ($y=0.5$).

The equations are given as

$$\nabla^2\psi = w$$

$$\frac{\partial w}{\partial t}+u\frac{\partial w}{\partial x}+v\frac{\partial w}{\partial y}=Pr\nabla^2 w+Ra\,Pr\frac{\partial T}{\partial x} \tag{47}$$

$$\frac{\partial T}{\partial t}+u\frac{\partial T}{\partial x}+v\frac{\partial T}{\partial y}=\nabla^2 T$$

where T, Pr and Ra are the temperature, Prandtl number and Rayleigh number, respectively. Equation (47) is subjected to the initial condition

$$w=T=0 \tag{48}$$

The no-slip boundary conditions of the velocity at boundary walls are assumed. Temperature has Dirichlet-type boundary conditions as 1 and 0 at the left and right walls of the cavity $[0,1]\times[0,1]$, whereas adiabatic conditions $\partial T/\partial y=0$ are imposed on the top and bottom. The proposed coupled numerical algorithm is applied to determine the stream function, vorticity and temperature variations with the given initial values iteratively.

In Figure 10 we present streamlines, vorticity and temperature contours at steady state for $Ra=10^3$, 10^4 and 10^5 with the constant boundary elements $N=48$, 64 and 100, respectively. As Rayleigh number increases, the boundary layer formation starts for all the variables stream function, vorticity and isotherms near the walls $x=0$ and 1. It is also observed from isotherms that the temperature contours undergo an inversion at the central region of the cavity. The primary vortex of the streamlines tends to separate and form two vortices through the corners $(0,1)$ and $(1,0)$ as the Rayleigh number increases. These behaviours are in good agreement with the previously

DOI: 10.1002/fld

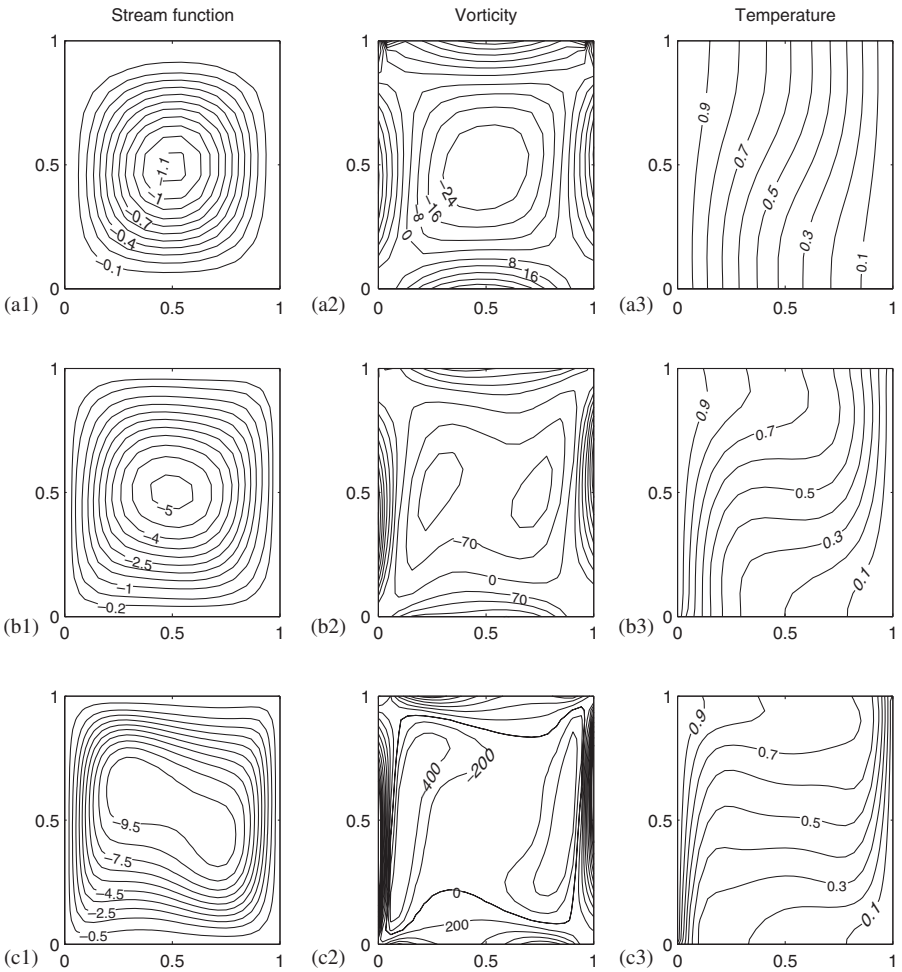

Figure 10. Stream function, vorticity and temperature contours: (a1–a3) $Ra=10^3$, $N=48$, $M=3$; (b1–b3) $Ra=10^4$, $N=64$, $M=2$; and (c1–c3) $Ra=10^5$, $N=100$, $M=2$.

Table I. Numerical results of natural convection for $Ra=10^3, 10^4$ and 10^5.

	$Ra=10^3$		$Ra=10^4$		$Ra=10^5$	
	Nu_0	$\overline{Nu}$	Nu_0	$\overline{Nu}$	Nu_0	$\overline{Nu}$
DRBEM&DQM	1.118	1.105	2.274	2.352	4.376	4.369
Davis[31]	1.117	1.118	2.238	2.243	4.509	4.519

published results [21–23]. The obtained results indicate that the present method is capable of handling quite a high Rayleigh number without difficulties and with a considerable small number of mesh points.

DOI: 10.1002/fld

In Table I, the values of the Nusselt number on the vertical boundary at $x=0$, Nu_0, and the average Nusselt number throughout the cavity, $\overline{Nu}$, obtained by the present study are compared with the benchmark solution given by De Vahl Davis [31] for $Ra=10^3, 10^4$ and 10^5. As Rayleigh number increases, we need to take more boundary elements to obtain better accuracy. Although there are some differences in the values in Table I, the flow patterns obtained by the coupling of the DRBEM and DQM show no distinguishable difference.

5. CONCLUSION

The transient two-dimensional Navier–Stokes equations in stream function–vorticity form are solved using the DRBEM in spatial and DQM in time domains. The DQM discretization in time direction results in a system of linear algebraic equations, which gives the solution vector for vorticity at the required time levels at one stroke. The vorticity boundary conditions are computed using a finite difference formula, which uses both the boundary and the interior stream function values. The proposed numerical algorithm is also applicable for the solution to natural convection in a square cavity. It gives quite good accuracy with a considerable small number of mesh points in both space and time directions.

ACKNOWLEDGEMENTS

The support of the Scientific and Technical Research Council of Turkey is gratefully acknowledged.

REFERENCES

1. Skerget L, Rek Z. Boundary-domain integral method using a velocity–vorticity formulation. *Engineering Analysis with Boundary Elements* 1995; **15**:359–370.
2. Ramsak M, Skerget L. Mixed boundary elements for laminar flows. *International Journal for Numerical Methods in Fluids* 1999; **31**:861–877.
3. Ramsak M, Skerget L, Hribersek M, Zunic Z. A multidomain boundary element method for unsteady laminar flow using stream function–vorticity equations. *Engineering Analysis with Boundary Elements* 2005; **29**:1–14.
4. Sarler B, Kuhn G. Primitive variable dual reciprocity boundary element method solution of incompressible Navier–Stokes equations. *Engineering Analysis with Boundary Elements* 1999; **23**:443–455.
5. Sarler B, Perko J, Gobin D, Goyeau B, Power H. Dual reciprocity boundary element method solution of natural convection in Darcy–Brinkman porous media. *Engineering Analysis with Boundary Elements* 2004; **28**:23–41.
6. Florez WF, Power H. DRM multidomain mass conservative interpolation approach for the BEM solution of the two-dimensional Navier–Stokes equations. *Computers and Mathematics with Applications* 2002; **43**:457–472.
7. Rahaim P, Kassab AJ. Pressure correction DRBEM solution for heat transfer and fluid flow in incompressible viscous fluids. *Engineering Analysis with Boundary Elements* 1996; **18**(4):265–272.
8. Power H, Mingo R. The DRM subdomain decomposition approach to solve the two-dimensional Navier–Stokes system of equations. *Engineering Analysis with Boundary Elements* 2000; **24**:107–119.
9. Power H, Mingo R. The DRM sub-domain decomposition approach for two-dimensional thermal convection flow problems. *Engineering Analysis with Boundary Elements* 2000; **24**:121–127.
10. Ingber MS, Kempka SN. A Galerkin implementation of the generalized Helmholtz decomposition for vorticity formulations. *Journal of Computational Physics* 2001; **169**:215–237.
11. Brown MJ, Ingber MS. Parallelization of a vorticity formulation for the analysis of incompressible viscous fluid flows. *International Journal for Numerical Methods in Fluids* 2002; **39**:979–999.
12. Ingber MS. A vorticity method for the solution of natural convection flows in enclosures. *International Journal of Numerical Methods for Heat and Fluid Flow* 2003; **13**(6):655–671.

DOI: 10.1002/fld

13. Zhao XY, Liao SJ. A short note on the general boundary element method for viscous flows with high Reynolds number. *International Journal for Numerical Methods in Fluids* 2003; **42**:349–359.
14. Wu Y, Liao S. Solving high Reynolds-number viscous flows by the general BEM and domain decomposition method. *International Journal for Numerical Methods in Fluids* 2005; **47**:185–199.
15. Sahin M, Owens RG. A novel fully implicit finite volume method applied to lid-driven cavity problem—part I: high Reynolds number flow calculations. *International Journal for Numerical Methods in Fluids* 2003; **42**:57–77.
16. Wu JS, Shao YL. Simulation of lid-driven cavity flows by parallel lattice Boltzmann method using multi-relaxation-time scheme. *International Journal for Numerical Methods in Fluids* 2004; **46**:921–937.
17. Wong JCF, Chan MKH. A consistent splitting scheme for unsteady incompressible viscous flows I. Dirichlet boundary condition and applications. *International Journal for Numerical Methods in Fluids* 2006; **51**:385–424.
18. Erturk E, Corke TC, Gökçöl C. Numerical solutions of 2-D incompressible driven cavity flow at high Reynolds numbers. *International Journal for Numerical Methods in Fluids* 2005; **48**:747–774.
19. Sousa E, Sobey IJ. Effect of boundary vorticity discretization on explicit stream-function vorticity calculations. *International Journal for Numerical Methods in Fluids* 2005; **49**:371–393.
20. Ghadi F, Ruas V, Wakrim M. Numerical solution of the time-dependent incompressible Navier–Stokes equations by piecewise linear finite elements. *Journal of Computational and Applied Mathematics* 2008; **215**(2):429–437.
21. Lo DC, Young DL, Tsai CC. High resolution of 2D natural convection in a cavity by the DQ method. *Journal of Computational and Applied Mathematics* 2007; **203**:219–236.
22. Ding H, Shu C, Yeo KS, XU D. Development of least-square-based two dimensional finite-difference schemes and their application to simulate natural convection in a cavity. *Computers and Fluids* 2004; **33**:137–154.
23. Shu C, Xue H. Comparison of two approaches for implementing stream function boundary conditions in DQ simulation of natural convection in a square cavity. *International Journal of Numerical Methods for Heat and Fluid Flow* 1998; **19**:59–68.
24. Kobayashi MH, Pereira JM. A computational stream function method for two-dimensional incompressible viscous flows. *International Journal for Numerical Methods in Engineering* 2005; **62**:1950–1981.
25. Shu C. *Differential Quadrature and its Applications in Engineering*. Springer-Verlag London Limited: Berlin, 2000.
26. Bozkaya C. Least squares differential quadrature time integration scheme in the DRBEM solution of convection–diffusion problems. *Engineering Analysis with Boundary Elements* 2007; **31**:83–93.
27. Bozkaya C, Tezer-Sezgin M. Boundary element solution of unsteady MHD duct flow with differential quadrature time integration scheme. *International Journal for Numerical Methods in Fluids* 2006; **51**:567–584.
28. Brebbia CA, Dominguez J. *Boundary Elements an Introductory Course*. Computational Mechanics Publications: Southampton, Boston, 1992.
29. Shu C, Richards BE. Application of generalized differential quadrature to solve two-dimensional incompressible Navier–Stokes equations. *International Journal for Numerical Methods in Fluids* 1992; **15**:791–798.
30. Ghia U, Ghia N, Shin CT. High-Re solutions for incompressible flow using the Navier–Stokes equations and a multigrid method. *Journal of Computational Physics* 1982; **48**:387–411.
31. De Vahl Davis G. Natural convection of air in a square cavity: a benchmark numerical solution. *International Journal for Numerical Methods in Fluids* 1983; **3**:249–264.

DOI: 10.1002/fld